Oxidative dimerization in metallothionein is a result of intermolecular disulphide bonds between cysteines in the α-domain

Klaus ZANGGER*[1], Gong SHEN†, Gülin ÖZ*, James D. OTVOS† and Ian M. ARMITAGE*[2]

*Department of Biochemistry, Molecular Biology and Biophysics, University of Minnesota, 6–155 Jackson Hall, 321 Church Street, Minneapolis, MN 55455, U.S.A., and †Department of Biochemistry, North Carolina State University, Polk Hall, PO Box 7622, Raleigh, NC 27695, U.S.A.

Upon storage under aerobic conditions metallothioneins (MTs) form a new species, which is characterized by a molecular mass approximately twice the size of monomeric MT and shifted $^{113/111}$Cd- and ^{1}H-NMR resonances. The investigation of this oxidative dimerization process by NMR spectroscopy allowed us to structurally characterize this MT species that has been described to occur *in vivo* and might be synthesized under conditions of oxidative stress. The oxidative dimer was characterized by the formation of an intermolecular cysteine disulphide bond involving the α-domain, and a detailed analysis of chemical shift changes and intermolecular nuclear Overhauser effects points towards a disulphide bond involving Cys^{36}. In contrast to the metal-bridged (non-oxidative) dimerization, the metal–cysteine cluster structures in both MT domains remain intact and no conformational exchange or metal–metal exchange was observed. Also in contrast to the many recently reported oxidative processes which involve the β-domain cysteine groups and result in the increased dynamics of the bound metal ions in this N-terminal domain, we found no evidence for any increased dynamics in the α-domain metals following this oxidation. Therefore these findings provide additional corroboration that metal binding in the C-terminal α-domain is rather tight, even under conditions of a changing cellular oxidation potential, compared with the more labile/dynamic nature of the metals in the N-terminal β-domain cluster under similar conditions.

Key words: ^{111}Cd NMR, ^{113}Cd NMR, metallothionein, NMR, oxidative dimerization.

INTRODUCTION

Metallothioneins (MTs) are a class of small (6–7 kDa) intracellular cysteine-rich (30 %) proteins with the highest known metal content after ferritins. MTs bind both essential (Cu^{+} and Zn^{2+}) and non-essential (Cd^{2+} and Hg^{2+}) metals. Metal binding in MTs has a high thermodynamic, but low kinetic stability. Thus metal binding is very tight, but there is facile metal exchange with other proteins. The binding of divalent metals such as Cd^{2+} occurs in two separate domains in mammalian MTs. The N-terminal β-domain, residues 1–30, binds three metals in a Cd_3S_9 cluster, whereas a 4-metal cluster, Cd_4S_{11}, is formed in the C-terminal α-domain (residues 31–61). The structures of the MT isoforms MT2 and MT1 from various mammalian sources, as obtained by NMR spectroscopy and X-ray crystal structure analysis, have been reported [1–4].

MTs are ubiquitous proteins, found in animals, higher plants, eukaryotic organisms and some prokaryotes. In mammals, the two major MT isoforms, MT1 and MT2, are most abundant in parenchymatous tissues, i.e. liver, kidney, pancreas and intestines, but their occurrence and biosynthesis have been documented in many tissues and cell types [5,6]. MTs are thought to function biologically as intracellular distributors and mediators of the metals they bind, and they seem to also play a fundamental role in heavy metal detoxification [5,6]. However, despite the fact that MTs have been investigated for over 40 years, no clear physiological role has been unambiguously assigned to this protein family [7], and the question remains as to the functional significance associated with the two distinct mammalian metal clusters contained in the separate protein domains. A series of studies by Vallee, Maret and co-workers [8–12] on the redox state dependence of the amount of zinc bound to MT has attracted much attention. They have shown that an oxidoreductive mechanism modulates the affinity of zinc for the cysteine thiolate ligands and the key players are GSH, GSSG and other oxidizing agents [10]. In this way, the cysteines of the metal thiolate clusters confer redox sensitivity to an otherwise redox-inert metal ligand (e.g. Zn^{2+}), and facilitate the potential for MT to participate in intracellular signal-transduction pathways [12]. Another redox-sensitive process, which leads to the formation of disulphide bonds, is the oxidation brought about by NO to form nitrosothiols, –SNO [13], which are subsequently converted to intramolecular Cys-S–S-Cys disulphides apparently specific to within the β-domain of mammalian MT1 [14]. In this latter case, the concomitant complete release of zinc from the β-domain has been postulated to be the basis for an anti-inflammatory role of MTs [14].

It has been noted for many years in our laboratories that samples of Cd_7-MT are not stable during long-term storage in aerobic conditions as seen from the appearance of additional signals in the $^{113/111}$Cd-NMR spectra [15], as well as an additional peak indicative of dimerization in gel-filtration analysis. Although the nature of the reaction leading to the production of this dimeric species was not investigated in detail, it was found to be partially, but not completely, reversed by the addition of thiol reagents. On this basis, it was suggested to be oxidative in nature and to involve the formation of intermolecular disulphide cross-links between one or more cysteine residues [16]. Dimerization could also be brought about by the addition of excess Cd^{2+} to a concentrated Cd-MT solution in the presence of phosphate [17–20]. This observation led to the description of a non-oxidative dimerization process, characterized by metal bridging of MT monomers.

The physiological significance of oxidative dimerization of MTs is unclear. Nevertheless, several studies have detected *in vivo* oxidative MT dimers after animals were exposed to high

Abbreviations used: MT, metallothionein; DTT, dithiothreitol; HMQC, heteronuclear multiple quantum correlation; NOE, nuclear Overhauser effect.

[1] Present address: Institute of Chemistry, University of Graz, Heinrichstrasse 28, A-8010 Graz, Austria.
[2] To whom correspondence should be addressed (e-mail armitage@bscl.msi.umn.edu).

levels of Cd [21,22]. Other studies have shown that Cd, especially in the presence of MT, may play a role in production of reactive oxygen species resulting in oxidative stress [23–25]. Moreover, there is evidence for the involvement of MTs in the response to oxidative stress [26,27]. Therefore, oxidative dimerization of MTs is likely to occur *in vivo* under stress conditions such as exposure to high levels of toxic metals or reactive oxygen species, and in a number of neurological disorders, including Alzheimer's disease, Parkinson's disease and amyotrophic lateral sclerosis, that have all been associated with oxidative stress [28]. In addition, the oxidative dimerization of MT might well play an important role in the newly discovered role of MTs as oxido-reductive mediators in signal-transduction pathways [10,12]. In this paper, we have structurally characterized the oxidized mammalian MT dimer.

EXPERIMENTAL

Mouse Cd_7-MT1 was prepared as described previously [4]. Zn-MTs were isolated from rabbit livers subjected to daily injections of 0.15 M $ZnSO_4$ for 6 days to give a total dose of 0.4 mmol of Zn^{2+}/kg of body mass. 6 h after the final injection, the animals were killed, and the livers removed and immediately frozen at −70 °C. To isolate Zn-MT, a single liver (approx. 100 g) was thawed and homogenized in a 1 litre blender with 150 ml of 5 mM Tris/HCl, pH 8.6, containing 0.25 M sucrose and 0.04 % β-mercaptoethanol. The homogenate was then centrifuged at 95000 ***g*** at 4 °C for 90 min. The supernatant was subsequently loaded on to a Sephadex G-75 column (120 cm × 10 cm) and eluted at a flow rate of 4 ml/min with 5 mM Tris/HCl, pH 8.6, and 0.02 % NaN_3. The MT-containing fractions were monitored for their Zn content with a Perkin–Elmer 3100 atomic absorption spectrometer. The MT-containing fractions were pooled and further purified on an anion exchange column (Whatman DE-32) equilibrated with 5 mM Tris/HCl, pH 8.6. A linear Tris/HCl gradient (5–200 mM, pH 8.6) was used for elution at a flow rate of 1.5 ml/min. Under these conditions, two peaks corresponding to Zn-MT1 and Zn-MT2 were separated. The pooled fractions for each isoform were concentrated in an Amicon apparatus using a YM2 membrane to a final concentration of approx. 0.3 mM. Dimers were obtained by storing a sample of 1.1 mM mouse Cd_7-MT1 in 10 mM Tris/HCl, pH 8.6, at 4 °C under aerobic conditions for 2 months.

To convert dimers back to monomers, a 40-fold molar excess of dithiothreitol (DTT) in the same buffer was added to the dimer sample and stored overnight at 4 °C. The sample was then loaded on to a Sephadex G-75 column (100 cm × 2.5 cm) and run at a flow rate of 0.4 ml/min. Approx. 90–95 % of the dimerized protein was converted back to the monomeric state using this procedure.

To quantify MT concentrations, the UV absorbance at 220 nm and pH 2, where the metals are completely removed, was used. Under these conditions the molar absorption coefficient is 47300 $M^{-1} \cdot cm^{-1}$ [29]. HPLC separations were performed using either a Bio-Rad 700 HPLC instrument or an Isco HPLC system (Lincoln, NE, U.S.A.) consisting of a pump (model 2350), a gradient programmer (model 2360) and an UV-Vis detector (model V4). Size-exclusion HPLC was performed with a semi-preparative GPC-60 column (300 mm × 7.8 mm; SynChrom, Darien, IL, U.S.A.) using 25 mM potassium phosphate buffer containing 100 mM KCl, pH 6.8, at a flow rate of 1 ml/min, or with an analytical GPC-100 column (250 mm × 4.6 mm; SynChrom) using 10 mM potassium phosphate buffer, pH 8.6, at a flow rate of 0.5 ml/min. Samples (10 μl) were applied and the eluate was monitored at a wavelength of 229 nm.

^{111}Cd-NMR spectra were acquired on a General Electric GN-500 MHz spectrometer using a 10 mm broad band probe, and all other NMR experiments were performed on a Varian Unity INOVA 600 MHz NMR spectrometer using either a 5 mm triple resonance probe for homonuclear proton spectra or a 5 mm inverse HCX probe tuned to the frequency of ^{113}Cd (133 MHz) for two-dimensional ^{1}H–^{113}Cd heteronuclear multiple quantum correlation (HMQC) experiments [30]. The ^{113}Cd-NMR spectra were referenced relative to an external 0.1 M solution of $Cd(ClO_4)_2$, and the proton spectra were referenced relative to the temperature corrected chemical shift of the residual solvent line [31]. All data processing was carried out with Vnmr 6.1a. Details of the processing schemes are given in the Figure legends.

RESULTS AND DISCUSSION

A solution of MT at millimolar concentrations stored under aerobic conditions at room temperature (25 °C) gradually produces a new species that elutes on a gel-filtration column with a retention time characteristic of a molecule approximately twice the molecular mass of freshly isolated MT. The proportion of the protein that elutes as the dimeric species increases with time in storage, from approx. 10 % after 11 days to approx. 50 % after 23 days. Evidence that the dimeric species represents covalently aggregated MT that is not reversible by dilution was provided by diluting the 23 day sample to 5 μM followed by storage overnight. Re-analysis by size-exclusion chromatography gave the same profile as seen before dilution. Even upon further dilution down to 0.2 μM, no difference in retention time was observed. In

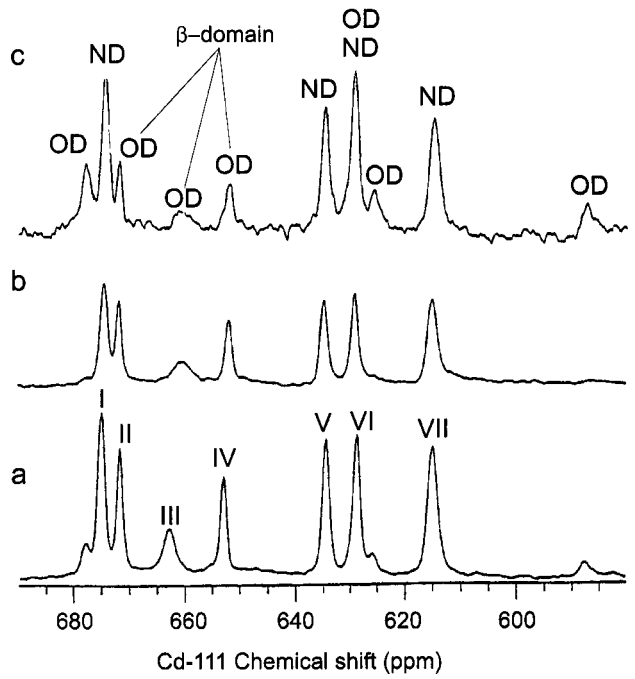

Figure 1 ^{111}Cd-NMR spectra (106 MHz) of monomeric and dimeric ^{111}Cd-MT2

^{111}Cd-MT2 (2.5 mM) was stored aerobically in 10 mM Tris/HCl, pH 8.6, at 4 °C for 10 days before acquiring spectrum (**a**). After an additional 11 days, the monomeric and dimeric species were separated by semi-preparative GPC-60 size-exclusion HPLC and then ultrafiltered to a concentration of approx. 1 mM. The spectrum in (**b**) is that of the isolated monomer fraction and (**c**) of the isolated dimer. Peaks in (**c**) are identified as originating from oxidative dimer (OD), or non-oxidative dimer (ND). Signals belonging to the N-terminal β-domain are indicated.

Table 1 Metal/protein and sulphydryl/protein ratios

M^{2+}, metal; SH, sulphydryl.

MT state	$[M^{2+}]/[MT]$	[SH]/[MT]
Monomer	7.0 ± 0.2	20.1 ± 0.3
Oxidative dimer	6.3 ± 0.2	18.6 ± 0.3
Non-oxidative dimer	10.0 ± 0.2	19.8 ± 0.3

contrast, a monomeric sample of 5 μM MT exhibited no observable dimerization even after 35 days of storage under aerobic conditions. These results provide clear evidence that, as would be expected for a reaction involving bimolecular association, dimerization is promoted at higher protein concentrations.

Since approximately one-third of the amino acid residues in MTs are cysteines, the most obvious mechanism for dimerization would be the formation of intermolecular disulphide bond(s) as a result of oxidation of the protein. To investigate the role of oxygen in MT oligomerization, a 2 mM Zn-MT2 sample was prepared and one half of this sample was stored aerobically and the other half anaerobically for 6 days before being analysed by size-exclusion HPLC. The results showed that approx. 40 % of the MT dimerized during aerobic incubation, and less than 10 % during anaerobic storage. Thus the presence of oxygen significantly influences the rate and/or extent of the dimerization reaction, and supports the hypothesis that MT molecules are cross-linked by cysteine disulphide bond(s). If dimerization were caused by cysteine oxidation, one would expect that this reaction could be reversed by the addition of thiol-reducing reagents. To test this prediction, the 2 mM Zn-MT2 sample that had been stored aerobically for 6 days was first diluted to 50 μM with 10 mM Tris/HCl, pH 8.6. To one half of this sample, DTT was added to give a 40-fold molar excess (2 mM). No DTT additions were made to the other half of the sample. Both aliquots were stored overnight at 4 °C and then analysed by size-exclusion HPLC. The results showed that approx. 90–95 % of the dimer could be converted back into the monomeric protein by incubation with DTT. Use of a greater excess of DTT and/or longer incubation times gave similar results. Since the percentage of dimers converted back to monomers is higher than the amount of oxidative dimers, the treatment with reducing thiols obviously also partly reverses the dimerization of the metal-bridged MT. Whereas the metal-bridged dimerization is only partially reversed by the DTT treatment, the oxidative dimers can be quantitatively converted to monomer as shown by the observable differences in NMR spectra (see below).

It should be noted that the use of different MT isoforms (MT1 and MT2) from different mammalian sources (mouse and rabbit) leads to the formation of the same dimeric species as shown by the experimental procedures described below. In addition, a variation in temperature only influenced the time course of the dimerization reaction, but not the chemical nature of the product formed.

To gain further insight into the mechanism and structure of the oxidative dimer, we used $^{111/113}$Cd- and ^{1}H-NMR spectroscopy. A number of changes were observed in the $^{111/113}$Cd-NMR spectra of MT upon the formation of dimers under aerobic conditions. As first described by Otvos et al. [15], three additional peaks appear in the ^{111}Cd-NMR spectrum (Figure 1) together with a decrease in the intensity of the Cd signals

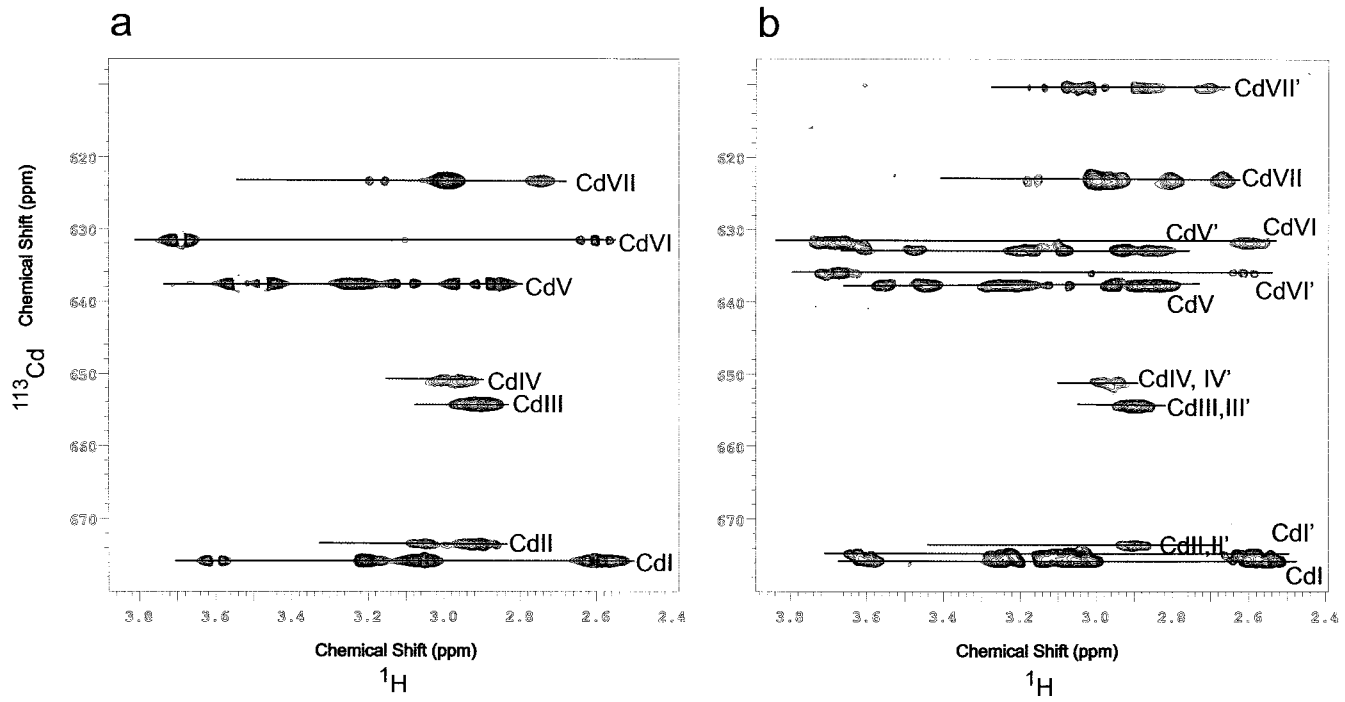

Figure 2 ^{1}H–^{113}Cd HMQCs of mouse $^{113}Cd_7$-MT1 of monomeric protein (a) and a sample stored under aerobic conditions for 2 months (b)

Both spectra were optimized for Cd–H coupling constants of 40 Hz and 32 scans of 2048 data points were acquired for each of the 128 increments. Prior to Fourier transformation, the data were multiplied by a 60°-phase-shifted squared sine-bell window function in both dimensions and zero filled to a final matrix of 2048 × 1024 complex points. Cd signals attributed to oxidative dimers are labelled as CdI′, CdII′, CdIII′, CdIV′, CdV′, CdVI′ and CdVII′.

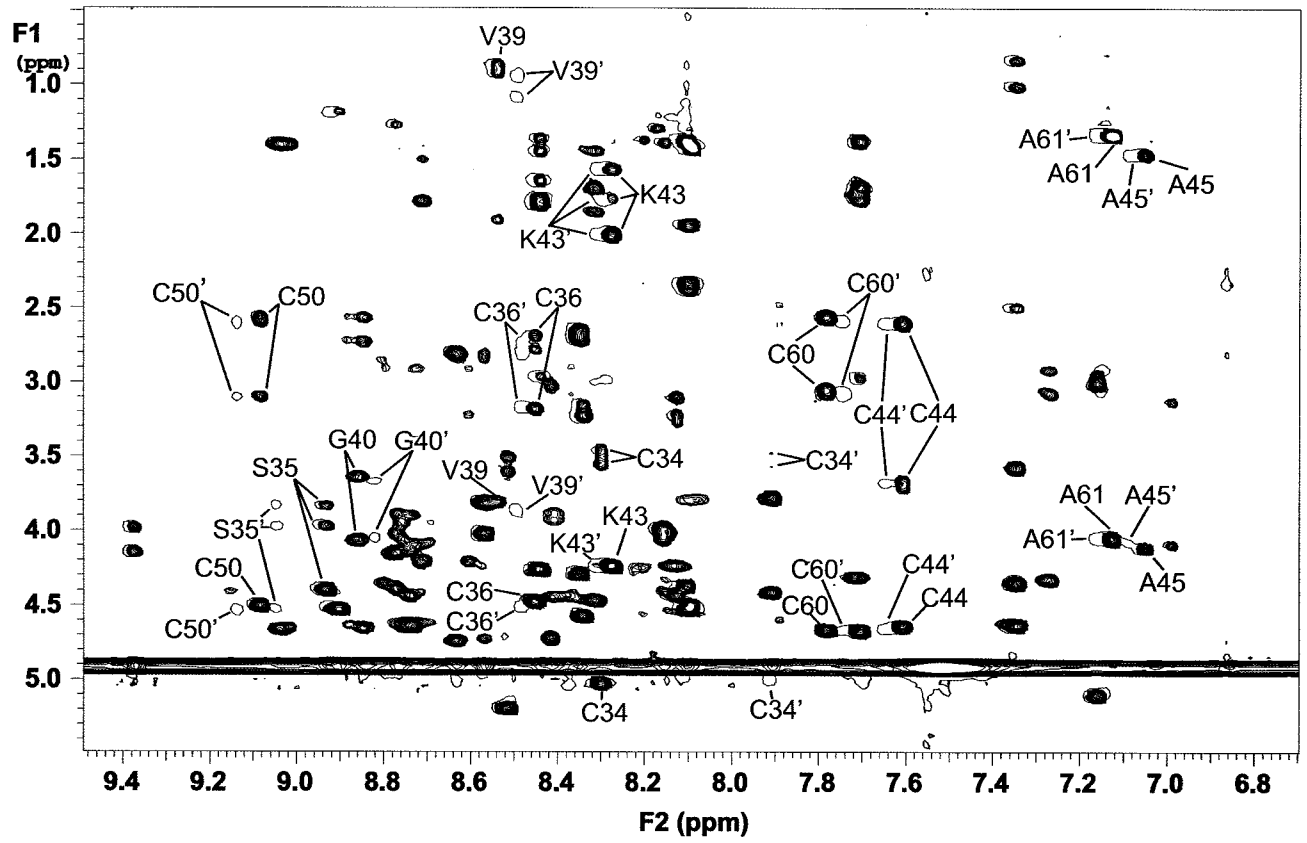

Figure 3 Fingerprint region of the 800 MHz TOCSY spectra of monomeric mouse Cd_7-MT1 (displayed as multiple contour levels) and a sample containing oxidative dimers in addition to non-oxidative dimers and monomers (with only 2 contour levels)

Peaks attributed to the oxidative dimer are indicated with an apostrophe (').

belonging to the β-domain. Monomers and dimers were separated on a GPC-60 column and the Cd spectra of the pooled fractions belonging to monomer and dimer are shown in Figures 1(b) and 1(c) respectively. The ^{111}Cd-NMR spectrum of the monomer fraction contains the expected seven resonances with approximately equal intensities for the signals from the α-domain and slightly lower intensities for the Cd peaks from the β-domain. However, the spectrum of the dimer shows more than seven peaks with widely varying intensities, but with all the peaks assigned to the 4-metal cluster showing a similar intensity. Since the possibility of contamination with a significant amount of monomer can be excluded, based upon the chromatographic evidence and the lower intensities of signals from the 3-metal cluster, the observed pattern can only be explained by the presence of two different types of dimeric species. The species that gave rise to shifted resonances at 678, 626 and 588 p.p.m. is derived from cysteine oxidation due to its reversibility in the presence of DTT. Metal-bridged (non-oxidative) dimers are characterized by unaltered signals from the α-domain and missing signals for the β-domain [15–18]. The variations in signal intensities can be explained by different amounts of oxidative and metal-bridged dimers with the latter lacking signals from the N-terminal β-domain. In Figure 1(c), peaks corresponding to the non-oxidative dimer are labelled ND and those originating from the oxidative dimer are labelled OD. These assignments are further corroborated by the fact that under anaerobic conditions only the peaks labelled ND (non-oxidative dimer) are found in the dimer fractions.

In an attempt to further characterize the chemical properties of these two dimeric forms, a careful analysis of the metal and thiol contents was carried out. The results of this analysis are shown in Table 1. The sample of oxidative dimer was prepared by storing a solution of 2 mM Zn-MT2 aerobically for 6 days and purification of the resulting dimer by HPLC. Some of this sample was presumably the non-oxidative dimer, judged by the failure to convert all of it back to monomer and the impossibility of separating non-oxidative and oxidative dimers. The non-oxidative dimer was prepared using the same procedure under anaerobic conditions. The monomeric sample was prepared from freshly isolated Zn-MT2. As expected, the monomeric sample showed the full complement of seven metal ions and 20 thiol groups. The lower number of thiol groups in the oxidative dimer is consistent with the proposal that it is formed by the oxidation of one cysteine thiolate group to form disulphide-bridged complexes. The role of excessive metals in the non-oxidative dimerization has been reported previously [17–20,32].

To further characterize the interaction between the subunits of the oxidative dimer, we acquired a ^{1}H–^{113}Cd-HMQC spectrum of partly dimerized mouse Cd_7-MT1, which is shown in Figure 2, together with the ^{1}H–^{113}Cd HMQC of a monomer sample. In addition to the degenerate ^{113}Cd α-domain signals known to arise from the monomer and non-oxidative dimer, the shifted ^{113}Cd

resonances for the α-domain oxidative dimer could be assigned on the basis of their correlations to sequentially assigned cysteine β-protons which show only minor shifts upon dimerization. Surprisingly, all of the proton–Cd connectivities in the monomer can also be found in the spectrum of the oxidative dimer with only minor reductions in the relative cross-peak intensities which precludes any significant release of bound Cd ions. The observation of all the expected Cd–Cys cross peaks from the two clusters in the oxidative dimer, therefore, implies that the metal–cysteine clusters remain intact as fast ($k > {}^{CdH}J$) Cd–Cd exchange would prohibit the evolution of anti-phase magnetization during a heteronuclear single-quantum correlation or HMQC experiment [33]. This is in contrast to the fast metal exchange and absence of ^{113}Cd resonances for the β-domain in metal-bridged dimers. The slightly reduced metal content of the oxidative dimer found by atomic absorption spectroscopy analysis (Table 1), therefore, might possibly be explained by the slightly increased metal exchange in the dimer β-domain.

What is most obvious in the ^{113}Cd-NMR spectrum of the oxidative dimer is the shift to a low frequency of Cd(VII). A low-frequency shift is indicative of a more shielded Cd nucleus, which could be achieved with fewer terminal and more bridging cysteines co-ordinating the metal [34,35]. Cd(VII) is bonded to just one terminal cysteine (Cys^{36}) in the monomer and the formation of a disulphide bond between this cysteine and another sulphur would convert the only terminal thiolate ligand at Cd(VII) to a bridging one which could be the cause for the observed shift to low frequency. Another, although less significant, shift to low frequency is observed for Cd(V) which could be caused by the involvement of either Cys^{33} or Cys^{48} in a disulphide bond, because both of these cysteines are connected to Cd(V) terminally and would offer the possibility for disulphide-bond formation. On the contrary, the shift to high frequency of Cd(VI) is indicative of a deshielding around this nucleus, which could be caused by converting bridging thiol ligands to terminal ones. Cd(VI) has three bridging ligands (Cys^{37}, Cys^{44} and Cys^{60}), however, the conversion of any of these to a terminal cysteine would break a Cd–Cys bond and all ^{113}Cd–^{1}H-HMQC cross peaks observed in the monomer are also found in the dimer. Based solely on the observed ^{113}Cd-NMR shifts of the oxidative dimer, the most likely intermolecular disulphide bond would involve Cys^{36}, which is the only terminal thiol ligand of Cd(VII), although the formation of disulphide bonds involving Cys^{33}or Cys^{48} cannot be excluded from the ^{113}Cd-NMR chemical-shift results.

Since there is just one signal observed for each Cd attributed to the oxidative dimer, it has to be symmetric. Anti-symmetric dimerization would be expected to lead to two shifted positions for each Cd signal. In addition, anti-symmetric dimerization offers the possibility of forming higher aggregates, by extending the process of intermolecular disulphide bond formation in a chain-like fashion. However, only a small amount of a higher molecular mass compound was found upon separation by gel filtration.

Further hints about the interaction interface come from the inspection of the proton chemical shifts in the monomer and dimer. The two-dimensional TOCSY [36] spectrum of the mixture of monomer and dimer (oxidative and metal bridged) overlaid with a spectrum of only the monomer is shown in Figure 3. The ^{113}Cd spectrum from the metal-bridged dimers of MT showed no changes for the resonances from the α-domain, but significantly reduced peak intensities for the β-domain ^{113}Cd resonances [17–20,32,37]. Therefore, the doubling of the ^{1}H cross peaks from the α-domain in Figure 3 must be correlated with the shifting of the α-domain ^{113}Cd-NMR resonances arising from the oxidative dimer. The most obvious differences in chemical shifts are reported in Table 2. Perhaps surprisingly, the cysteine β-protons are shifted less significantly than some of the corresponding cysteine amide signals. The shifting of the backbone NH signals, however, is most sensitive to changes in the H-bonding pattern or solvent accessibility [38] and much less to changes in the co-ordination involving side-chain atoms of that amino acid. A spatial arrangement of the atoms, protons and Cd ions, exhibiting changes in chemical shifts is shown in Figure 4, where the size of the spheres correspond to the absolute magnitude of the change in chemical shift. The largest shifts in the cysteine side-chain protons occurs for Cys^{36} and a general clustering of proton shifts is found around Cd(VII), which also shows the largest ^{113}Cd chemical shift. Both Cys^{33} and Cys^{48}, which might be implicated in the oxidative dimerization process based on the observed change in Cd(V), show no changes in ^{1}H chemical shifts.

Table 2 Changes in ^{113}Cd- and ^{1}H-NMR chemical shifts upon the formation of oxidative dimers

Signal	$\Delta(\delta_{monomer} - \delta_{dimer})$ (p.p.m.)
Cd	
Cd(I)	−0.7
Cd(V)	5.1
Cd(VI)	−4.0
Cd(VII)	12.9
NH	
Cys^{34}	0.39
Ser^{35}	−0.12
Cys^{36}	−0.03
Val^{39}	0.04
Gly^{40}	0.04
Lys^{43}	−0.03
Cys^{44}	−0.04
Ala^{45}	−0.03
Cys^{50}	−0.05
Cys^{60}	0.04
Ala^{61}	−0.03
Others	
Cys^{34}-α	0.02
Ser^{35}-α	−0.12
Cys^{36}-α	−0.04
Cys^{36}-βs	0/−0.03
Val^{39}-γs	−0.07/−0.1
Cys^{50}-α	−0.02

Unambiguous identification of the dimer interface would be provided by intermolecular nuclear Overhauser effects (NOEs). However, the interpretation of nuclear Overhauser enhancement spectra from the dimer is complicated both by the broader lines and the presence of metal-bridged dimers, which cannot be separated from the oxidative dimers. Therefore Cys^{37}-NH···Asp^{55}-NH, Gly^{40}-NH···Asp^{55}-NH, Lys^{43}-γH···Val^{49}-γH, Lys^{43}-NH···Lys^{56}-γH, Lys^{43}-NH···Cys^{59}-αH are the only NOEs involving shifted resonances which appear upon the formation of dimers under aerobic conditions that could be unambiguously assigned to the oxidative dimer. These NOEs involve residues near the C-terminal end of MT and are spatially close to Cys^{36}. The low number of intermolecular NOEs prohibited an analysis of the interaction interface using molecular modelling. However, a rough model of the oxidative dimer could be created based upon the observed shifts (Cd and protons) and the observed NOEs. We assumed that the oxidative dimers were formed by an intermolecular disulphide bond between the Cys^{36} residues on two MT molecules in a symmetric head–head type dimer, a

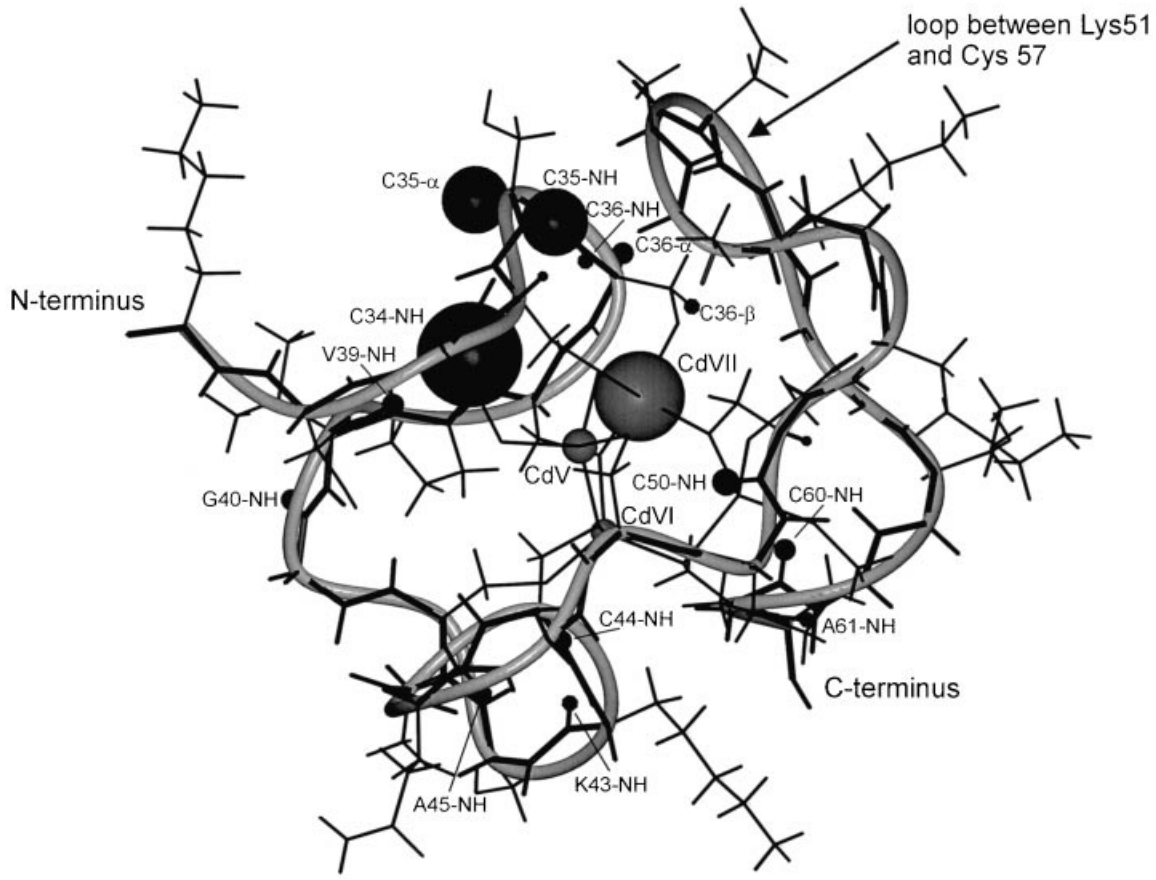

Figure 4 Structure of the α-domain of mouse MT1 (Protein DataBank accession number 1DFS) showing the positions of the NMR signals shifted upon the formation of oxidative dimers (see Table 2)

The relative sizes of the spheres indicate relative changes in chemical shifts for proton (black spheres) and Cd (grey spheres) resonances. A clustering of larger changes around the loop containing Cys^{36} can be seen. This Figure was made using MOLMOL [35].

possible model of which is shown in Figure 5. This model was based on the observed intermolecular NOEs (shown as black spheres) and the chemical shift differences. The loop between residues 51–57 appears to somehow 'protect' this Cys^{36} residue in mammalian MTs [1,2,4,39,40]. However, this loop is the least well-defined region in the α-domain for the NMR-derived MT structures [1,2,4,39,40], and it also has the highest B-factors in the crystal structure [39]. Therefore, dimerization could be facilitated by a slight opening of this loop. Maybe the most interesting finding of this study is the fact that the Cd ions bound in the C-terminal 4-metal cluster are not released upon the formation of the intermolecular disulphide-bond. The line widths of all seven Cd resonances do not even show any evidence for increased mobility of the metal bound in the oxidative dimer. This is in contrast to the increased metal mobility that is observed for the β-domain $^{113}Cd^{2+}$ ions in the metal-bridged dimers [17–20], following the reaction with the GSH/GSSG redox couple [9,10], or after the formation of intramolecular disulphides in this domain following the reaction with NO [13,14]. To the best of our knowledge, this is the only known case of an oxidative reaction occurring in the α-domain of MTs. As the low redox potential of MTs (−366 mV [9]) makes them a likely candidate for oxidative reactions *in vivo*, our results indicate that if such a reaction occurs in living cells [21,22], it does not lead to mobilization of metals bound to the α-domain. The different metal reactivity of the two domains and the different metal affinity associated with the two domains correlates well with the proposal that the α-domain plays a detoxification/sequestering role for toxic and/or excess metal ions. These findings thus contribute to the assignment of distinct and different functional roles to the two MT metal clusters which correlates with the varying metal exchange in the two domains. The proposed functional roles of the two domains in MTs are: N-terminal β-domain, an involvement in the homoeostasis of the essential metal ions [5,6] and, C-terminal α-domain, the tight binding/sequestration of excess and/or toxic metal ions [41,42].

In conclusion, we have traced the oxidative dimerization of MT to be caused by a symmetric head–head disulphide bond formation between Cys^{36} in two monomers. These oxidative dimers are formed *in vitro* by storage in aerobic conditions along with metal-bridged dimers, from which they cannot be chromatographically separated. However, these dimers can be distinguished in NMR spectra by shifts of the Cd and of some proton signals in the α-domain. As it was not possible to separate metal-bridged and oxidative dimers, we only used information from chemical shifts and NOEs from those signals that could be attributed unambiguously to the oxidative dimer to draw conclusions about the interface. Of note, however, is that in contrast to other reported oxidative processes in MTs which affect the metal stability in the β-domain, the formation of oxidative

Figure 5 Model of a symmetric head–head dimer showing spins involved in intermolecular NOEs as black spheres and the two Cys[36] residues as grey spheres

Two monomers of the rat MT2 X-ray structure (Protein DataBank accession number 4MT2) have been used for this model since this is the only MT for which the relative orientation of the two domains is known. This Figure was made using MOLMOL [35].

dimers does not lead to increased mobility of metals from either domain.

Partial support of this work comes from the National Institutes of Health grant DK18778 to I.M.A. K.Z. thanks the Austrian Fonds zur Förderung der wissenschaftlichen Forschung for an Erwin Schrödinger Fellowship (project number J-1618CHE). G.Ö. thanks the Graduate School at the University of Minnesota for a Louise T. Dosdall Fellowship. NMR instrumentation was provided with funds from the National Science Foundation (BIR-961477) and the University of Minnesota, Medical School.

REFERENCES

1 Arseniev, A., Schultze, P., Wörgötter, E., Braun, W., Wagner, G., Vašak, M., Kägi, J. H. and Wüthrich, K. (1988) Three-dimensional structure of rabbit liver [Cd_7]-metallothionein-2a in aqueous solution determined by nuclear magnetic resonance. J. Mol. Biol. **201**, 637–657
2 Messerle, B. A., Schäffer, A., Vašak, M., Kägi, J. H. and Wüthrich, K. (1990) Three-dimensional structure of human [$^{113}Cd_7$]-metallothionein-2 in solution determined by nuclear magnetic resonance spectroscopy. J. Mol. Biol. **214**, 765–779
3 Robbins, A. H., McRee, D. E., Williamson, M., Collett, S. A., Xuong, N. H., Furey, W. F., Wang, B. C. and Stout, C. D. (1991) Refined crystal structure of Cd, Zn metallothionein at 2.0 Å resolution. J. Mol. Biol. **221**, 1269–1293
4 Zangger, K., Öz, G., Otvos, J. D. and Armitage, I. M. (1999) Three-dimensional solution structure of mouse [Cd_7]-metallothionein-1 by homonuclear and heteronuclear NMR spectroscopy. Protein Sci. **8**, 2630–2638
5 Kägi, J. H. and Kojima, Y. (1987) Chemistry and biochemistry of metallothionein. Experientia, Suppl. **52**, 25–61
6 Kägi, J. H. and Schäffer, A. (1988) Biochemistry of metallothionein. Biochemistry **27**, 8509–8515
7 Palmiter, R. D. (1998) The elusive function of metallothioneins. Proc. Natl. Acad. Sci. U.S.A. **95**, 8428–8430
8 Maret, W., Larsen, K. S. and Vallee, B. L. (1997) Coordination dynamics of biological zinc 'clusters' in metallothioneins and in the DNA-binding domain of the transcription factor Gal4. Proc. Natl. Acad. Sci. U.S.A. **94**, 2233–2237
9 Maret, W. and Vallee, B. L. (1998) Thiolate ligands in metallothionein confer redox activity on zinc clusters. Proc. Natl. Acad. Sci. U.S.A. **95**, 3478–3482
10 Jiang, L. J., Maret, W. and Vallee, B. L. (1998) The glutathione redox couple modulates zinc transfer from metallothionein to zinc-depleted sorbitol dehydrogenase. Proc. Natl. Acad. Sci. U.S.A. **95**, 3483–3488
11 Jacob, C., Maret, W. and Vallee, B. L. (1998) Control of zinc transfer between thionein, metallothionein, and zinc proteins. Proc. Natl. Acad. Sci. U.S.A. **95**, 3489–3494
12 Maret, W., Jacob, C., Vallee, B. L. and Fischer, E. H. (1999) Inhibitory sites in enzymes: zinc removal and reactivation by thionein. Proc. Natl. Acad. Sci. U.S.A. **96**, 1936–1940
13 Kröncke, K. D., Fehsel, K., Schmidt, T., Zenke, F. T., Dasting, I., Wesener, J. R., Bettermann, H., Breunig, K. D. and Kolb-Bachofen, V. (1994) Nitric oxide destroys zinc-sulfur clusters inducing zinc release from metallothionein and inhibition of the zinc finger-type yeast transcription activator LAC9. Biochem. Biophys. Res. Commun. **200**, 1105–1110
14 Zangger, K., Öz, G., Haslinger, E., Kunert, O. and Armitage, I. M. (2001) Nitric oxide selectively releases metals from the N-terminal domain of metallothioneins: potential role at inflammatory sites. FASEB J. **15**, 1303–1305
15 Otvos, J. D., Engeseth, H. R. and Wehrli, S. (1985) Preparation and ^{113}Cd NMR studies of homogeneous reconstituted metallothionein: reaffirmation of the two-cluster arrangement of metals. Biochemistry **24**, 6735–6740
16 Shen, G. (1995) Structural properties of metallothionein isoforms. Ph.D. thesis, Department of Biochemistry, North Carolina State University, Raleigh, NC, U.S.A.
17 Palumaa, P. and Vašak, M. (1992) Binding of inorganic phosphate to the cadmium-induced dimeric form of metallothionein from rabbit liver. Eur. J. Biochem. **205**, 1131–1135
18 Palumaa, P., Mackay, E. A. and Vašak, M. (1992) Nonoxidative cadmium-dependent dimerization of Cd_7-metallothionein from rabbit liver. Biochemistry **31**, 2181–2186
19 Palumaa, P., Zerbe, O. and Vašak, M. (1993) Formation and spectroscopic characterization of a novel monomeric cadmium- and phosphate-containing form of metallothionein. Biochemistry **32**, 2874–2879
20 Palumaa, P. and Vaher, M. (1996) Metal-induced dimerization of Cd_7-metallothionein. Role of anions. Ann. Clin. Lab. Sci. **26**, 264–268

21 Suzuki, K. T. and Yamamura, M. (1980) Isolation and characterization of metallothionein dimers. Biochem. Pharmacol. **29**, 689–692
22 Suzuki, K. T., Ohnuki, R. and Yaguchi, K. (1983) Post-mortem and *in vitro* dimerization of metallothionein in cadmium-accumulated rat liver and kidney. Toxicol. Lett. **16**, 77–84
23 Stohs, S. J. and Bagchi, D. (1995) Oxidative mechanisms in the toxicity of metal ions. Free Radical Biol. Med. **18**, 321–336
24 O'Brien, P. and Salacinski, H. J. (1998) Evidence that the reactions of cadmium in the presence of metallothionein can produce hydroxyl radicals. Arch. Toxicol. **72**, 690–700
25 Thevenod, F. and Friedmann, J. M. (1999) Cadmium-mediated oxidative stress in kidney proximal tubule cells induces degradation of Na^+/K^+-ATPase through proteasomal and endo-/lysosomal proteolytic pathways. FASEB J. **13**, 1751–1761
26 Sato, M. and Bremner, I. (1993) Oxygen free radicals and metallothionein. Free Radical Biol. Med. **14**, 325–337
27 Thornalley, P. J. and Vašak, M. (1985) Possible role for metallothionein in protection against radiation-induced oxidative stress. Kinetics and mechanism of its reaction with superoxide and hydroxyl radicals. Biochim. Biophys. Acta **827**, 36–44
28 Cuajungco, M. P. and Lees, G. J. (1997) Zinc metabolism in the brain: relevance to human neurodegenerative disorders. Neurobiol. Dis. **4**, 137–169
29 Bühler, R. H. and Kägi, J. H. (1979) Spectroscopic properties of zinc-metallothionein. Experientia, Suppl. **34**, 211–220
30 Live, D., Armitage, I. M., Dalgarno, D. C. and Cowburn, D. (1985) Two-dimensional ^1H-^{113}Cd chemical-shift correlation maps by ^1H-detected multiple-quantum NMR in metal complexes and metalloproteins. J. Am. Chem. Soc. **107**, 1775–1777
31 Wishart, D. S., Bigam, C. G., Yao, J., Abildgaard, F., Dyson, H. J., Oldfield, E., Markley, J. L. and Sykes, B. D. (1995) ^1H, ^{13}C and ^{15}N chemical shift referencing in biomolecular NMR. J. Biomol. NMR **6**, 135–140
32 Otvos, J. D., Engeseth, H. R., Nettesheim, D. G. and Hilt, C. R. (1987) Interprotein metal exchange reactions of metallothionein. Experientia, Suppl. **52**, 171–178
33 Krishnan, V. V. and Rance, M. (1995) Influence of chemical exchange among heteronuclear coherence-transfer experiments in liquids. J. Magn. Reson. **1161**, 97–106
34 Armitage, I. M. and Otvos, J. D. (1982) Principles and applications of ^{113}Cd NMR to biological systems. Biol. Magn. Reson. **4**, 79–144
35 Öz, G., Pountney, D. L. and Armitage, I. M. (1998) NMR spectroscopic studies of $I = 1/2$ metal ions in biological systems. Biochem. Cell Biol. **76**, 223–234
36 Jeener, J., Meier, B. H., Bachmann, P. and Ernst, R. R. (1979) Investigation of exhange processes by two-dimensional NMR spectroscopy. J. Chem. Phys. **71**, 4546–4563
37 Nettesheim, D. G., Engeseth, H. R. and Otvos, J. D. (1985) Products of metal exchange reactions of metallothionein. Biochemistry **24**, 6744–51
38 Cavanagh, J., Fairbrother, W. J., Palmer, A. G. and Skelton, N. J. (1996) Protein NMR Spectroscopy: Principles and Practice, p. 532, Academic Press, San Diego
39 Furey, W. F., Robbins, A. H., Clancy, L. L., Winge, D. R., Wang, B. C. and Stout, C. D. (1987) Crystal structure of Cd, Zn metallothionein. Experientia, Suppl. **52**, 139–148
40 Schultze, P., Wörgötter, E., Braun, W., Wagner, G., Vašak, M., Kägi, J. H. and Wüthrich, K. (1988) Conformation of $[Cd_7]$-metallothionein-2 from rat liver in aqueous solution determined by nuclear magnetic resonance spectroscopy. J. Mol. Biol. **203**, 251–268
41 Hamer, D. H. (1986) Metallothionein. Annu. Rev. Biochem. **55**, 913–951
42 Cherian, M. G., Howell, S. B., Imura, N., Klaassen, C. D., Koropatnick, J., Lazo, J. S. and Waalkes, M. P. (1994) Role of metallothionein in carcinogenesis. Toxicol. Appl. Pharmacol. **126**, 1–5

Received 10 April 2001/10 July 2001; accepted 7 August 2001